Journal of Archaeological Science: Reports 35 (2021) 102666

Contents lists available at ScienceDirect

Journal of Archaeological Science: Reports

journal homepage: www.elsevier.com/locate/jasrep

Fade to Black: The implications of Mount Maloney Black pottery from a Terminal Classic deposit, Cahal Pech, Belize, using a comparative multi-method compositional approach

John E. Douglas [a,*], Brandi L. MacDonald [b], Claire E. Ebert [c], Jaime J. Awe [d], Laure Dussubieux [e], Catherine E. Klesner [f]

[a] *Department of Anthropology, University of Montana, Missoula, Montana 59812, United States*
[b] *Archaeometry Laboratory, Research Reactor Center, University of Missouri, Columbia, MO 65211, United States*
[c] *Department of Anthropology, University of Pittsburgh, Pittsburgh, PA 15260, United States*
[d] *Department of Anthropology, Northern Arizona University, Flagstaff, AZ 86011, United States*
[e] *Elemental Analysis Facility, Field Museum, Chicago, IL 60605, United States*
[f] *Department of Materials Science and Engineering, University of Arizona, Tucson, AZ 87521, United States*

A R T I C L E I N F O

Keywords:
Terminal Classic Maya
Utility serving vessels
Identifying local interaction through ceramics
Slip composition using LA-ICP-MS
Paste composition using NAA
Intra-laboratory LA-ICP-MS analyses

A B S T R A C T

Excavations of a peri-abandonment deposit at Cahal Pech, a Classic Maya center in the Upper Belize Valley, showed an increase in Mount Maloney Black (MMB) ceramics compared with earlier Terminal Classic contexts. This change is intriguing because the type is closely associated with Xunantunich, a nearby political center. To explore the causes of this change, we characterized a sample of MMB sherds to identify their origins as a proxy for underlying regional interactions. We sampled MMB sherds from four locations: the peri-abandonment deposit, two peripheral localities in the Cahal Pech polity, and the Xunantunich epicenter. In total, 89 sherds were characterized, both for paste, using neutron activation analysis (NAA), and for slip composition, using laser ablation inductively coupled plasma mass spectrometry (LA-ICP-MS). The NAA study indicated that MMB sherds from Cahal Pech were produced locally, and included a paste group previously identified with Preclassic contexts at Cahal Pech, over a millennium earlier. The slip study was augmented by x-ray diffraction (XRD), scanning electron microscopy (SEM), and Raman spectroscopy, which provided additional information on the colorants, particle sizes, and homogeneity. The study expanded to include comparative characterization of a fine ware black slipped pottery type from a site north of the Belize Valley as a control. MMB slip recipes vary sufficiently to provide differentiation between recipes, and they partially pattern by locality. We conclude that the observed ceramic change likely relates to a narrowing, not an expansion, of exchange networks. This multi-method study, unique in the Maya lowlands, provides insight into ceramic production and exchange and charts new research directions.

1. Introduction

Characterization analyses of Maya ceramics play increasingly important roles in the study of ceramic production and regional interaction (Bishop, 1994, 2014; Callaghan et al., 2017, 2018; Ebert et al., 2019; Halperin and Bishop, 2016; Howie, 2005). Here we demonstrate the power of a focused characterization study that began with a utilitarian pottery type, Mount Maloney Black (MMB), from a single deposit. The context of the sherds relates to the abandonment of Cahal Pech, a medium-sized Classic period (250–900 CE) Maya center in the Upper Belize Valley (Fig. 1). This study presents a comparison of the ceramics from this deposit with those found at the nearby center of Xunantunich. The goal of determining the source of MMB was to test the nature of regional interaction that might relate to the abandonment of Cahal Pech as an elite center. Ultimately, this work provides a wide range of inferences concerning ceramic industries, stability, and change in the Upper Belize Valley during the Terminal Classic.

Beyond substantive contributions to Classic Maya studies, this

* Corresponding author.
E-mail addresses: john.douglas@umontana.edu (J.E. Douglas), macdonaldb@missouri.edu (B.L. MacDonald), C.Ebert@penn.edu (C.E. Ebert), Jaime.Awe@nau.edu (J.J. Awe), ldussubieux@fieldmuseum.org (L. Dussubieux), klesnerc@email.arizona.edu (C.E. Klesner).

https://doi.org/10.1016/j.jasrep.2020.102666
Received 19 June 2020; Received in revised form 23 October 2020; Accepted 6 November 2020
Available online 9 December 2020

project incorporates evaluation of two important methodological issues. First, we characterize 89 sherds for both slip and paste composition. No other study published in the Maya lowlands has focused on the chemical characterization of a single utilitarian ceramic type as thoroughly, using multiple methods. We show that in a region known for dispersed pottery production and often subtle geological variation, multiple lines of evidence can detect similarities and differences to document production and consumption between groups. Second, the study integrates and validates LA-ICP-MS data from two different laboratories, examining the potential for collaborative regional studies from multiple collections.

1.1. Archaeological background

From the Preclassic through Classic period, the Upper Belize Valley was the home to a network of Maya polities (Fig. 1) which competed and interacted for centuries, shifting in building activity levels and sociopolitical importance, but without one center gaining long-term dominance (Gaber, 2004; Helmke and Awe, 2012). Two well-known centers in the region, both publicly interpreted National Archaeological Reserves, are Cahal Pech, located at the confluence of the Macal and Mopan Rivers, and Xunantunich, in the Mopan River Valley. The sites are situated 9 km apart, yet possess distinct occupational histories. During the Terminal Classic, a phase widely placed at 750–900 CE in the Belize Valley, political and organizational trajectories are divergent between the two polities. Terminal Classic construction activities at the epicenter of Xunantunich are brisk and include the placement of stelae commemorating elite events at 820 and 849 CE (Helmke et al., 2010; LeCount et al., 2002). The expansion of elite activity in ninth century Xunantunich occurred while Cahal Pech's center rapidly dwindled: the elite abandoned the site's acropolis and the construction programs and maintenance of the structures and plazas possibly ended as early as 850 CE (Awe, 2013).

The ceramic type analyzed for this study, Mount Maloney Black (MMB), is long associated with the Late to Terminal Classic Maya occupation of the Upper Belize Valley (Gifford, 1976; LeCount, 2010). Large incurved bowls are the most common form (short-necked jars comprise most of the remainder of the assemblage), with crushed calcite temper in the paste and a black slip. The slip is "fugitive," easily flaking off the surface of most sherds. Functionally, MMB is a member of the household serving vessel category, a relatively stable and hallmark ceramic class in the Maya world. These are everyday items that, although not required for biological existence, served practical and social needs. Household serving vessels likely formed a middle ground in ceramic use-life and production: steady restocking was required, although use-life was longer than for cooking pots (Straight, 2017). Compositional studies of household ceramics within the Upper Belize Valley (Ebert et al., 2019; Garcia, 2008; Jordan et al., 2020) and at other medium-sized centers in the Classic Maya world (e.g., Howie, 2005:62) indicate that production by a network of part-time potters would likely have taken place locally. These ubiquitous archaeological items are also symbolically potent objects, meaningfully linked to sustenance, kinship, and home. They play important roles in peri-abandonment and other ritual deposits among the Maya (Awe et al., 2020a, 2020b; LeCount, 2010; LeCount, 1996).

1.1.1. Xunantunich perspectives

MMB was recognized as a dominant ceramic type at Xunantunich well before the type, and the site, had received their modern names (Thompson, 1942). It is found routinely in Spanish Lookout phase occupations —Late to Terminal Classic period—throughout the Upper Belize Valley, but the widespread substitution of black-slipped household serving vessels for the usual red-slipped ones (i.e. Vaca Falls and Garbutt Creek Red) occurs only at Xunantunich (Gifford, 1976). The role of MMB at Xunantunich has been given wide-ranging consideration by LeCount (1996, 2010) and her student (Garcia, 2008), who make three important points. First, the type changes through time; the microseriation of bowl lip forms accurately identify temporally distinct deposits during the Late to Terminal Classic. Additionally, LeCount (1996)

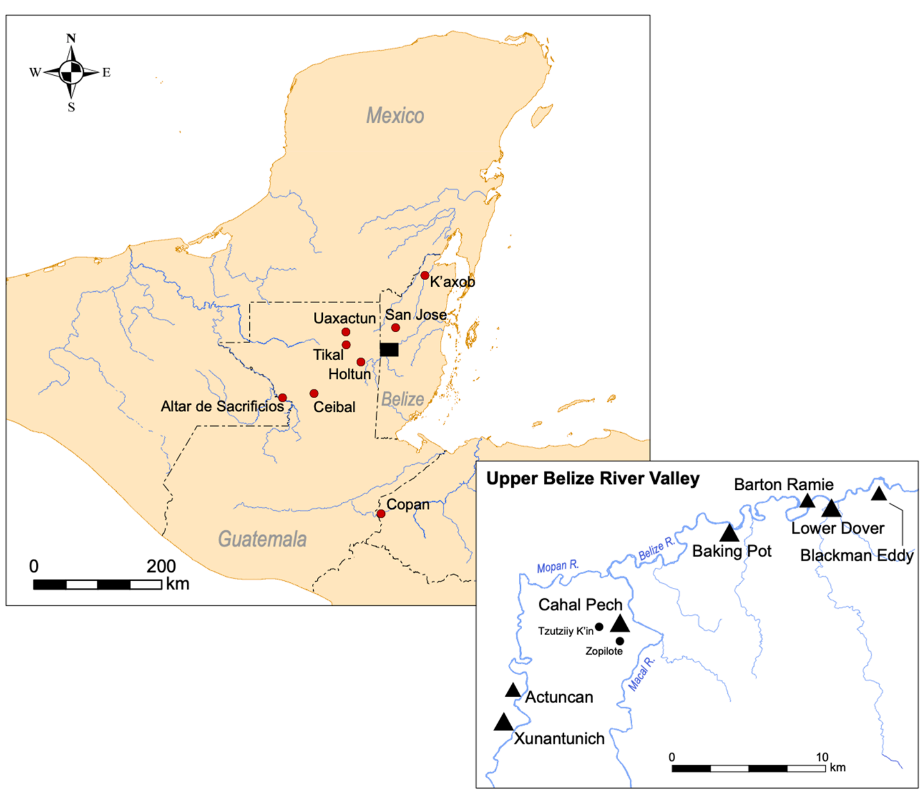

Fig. 1. Regional map showing the Belize River Valley (black rectangle), the San Jose site, and major Classic Maya lowland sites. Lower left shows the location of sampled locations in the Belize River Valley and other important sites.

found time-sensitive changes in the occurrence of certain unusual forms as well as a change in jar neck shapes. Second, thin section analysis indicates that MMB was produced with heterogenous paste recipes (Garcia, 2008) indicating dispersed, small-scale fabrication. Third, the uniqueness of these black slipped ceramics and their everyday context may have helped create a social identity that crosscut class divisions within the polity now known as Xunantunich (LeCount, 2010). The use of MMB also extends to ritual contexts, as noted by LeCount: "Mount Maloney bowls are also the most common vessels found in termination and dedication deposits at Xunantunich (1996:253–254)."

1.1.2. Cahal Pech perspectives

The most elaborate and best-studied Terminal Classic construction at Cahal Pech is Plaza H. Located on the acropolis at the entrance of the ceremonial center (Fig. 2), the plaza was built over an area that was lightly used during the Late Classic. There were two episodes of Terminal Classic construction, with the final four platforms, almost exclusively faced with unshaped stone, standing 30–50 cm above the plastered plaza floor. The downhill H-3 wall, defining the northern edge of the plaza, stood about 2 m high, making H-3, topped with a waddle and daub structure, inter-visible with farming communities in the Macal River Valley below. A vaulted tomb was built into the northeast structure, H-1, during the last Terminal Classic construction phase. The tomb contained a richly appointed male with elite grave offerings including 11 Spanish Lookout phase ceramic vessels, several jade items, and a necklace composed of teeth from at least 52 dogs (Awe, 2013:47). The burial is dated through multiple means: the ceramic assemblage, an AMS ^{14}C date, and stratigraphy. Plaza H was likely the residential compound of a ruling family, with the tomb commemorating the final known ruler of the Cahal Pech polity, diminished in power compared with his predecessors but with elements of Late Classic leadership (Awe, 2013; Douglas et al., 2015).

Immediately south of Structure H-1 and the tomb was a peri-abandonment deposit. Interpreted as representing activities associated with re-visitation and ancestor veneration, the deposit contained thousands of large ceramic sherds along with obsidian blades, large chert bifaces, mano and metate fragments, marine shell ornaments, fragmentary human and faunal remains, jade, a notched projectile point, a spindle whorl, and a bark beater. For most of Cahal Pech, a thin layer of sterile soil is found between Late Classic constructions and peri-abandonment deposits, suggesting a significant lapse between activities (Awe et al., 2020a), but the Plaza H deposit appears to rest directly on the plaza floor, consistent with a late abandonment. An AMS ^{14}C assay on a deer antler fragment dates the deposit to cal 770–950 CE (UCIAMS-174933; 1175 ± 15), whereas a deer phalange from the tomb dates to cal 770–890 CE (UCIAMS-174954; 1185 ± 15). Though a plateau in the calibration curve produced large calibrated date ranges at the 95% confidence interval for both dates, their central distribution (71–78% confidence intervals) closely fit temporal expectations: cal 800–890 CE for the tomb; cal 820–895 CE for the peri-abandonment deposit (OXCAL 4.4 with INTCAL20; Bronk Ramsey, 2009). The ten-year span between the uncalibrated dates for the tomb and the peri-abandonment deposit, alongside a limited amount of remodeling and accumulation found after the final construction phase in Plaza H, suggest that the two events are separated by a short time, likely best measured in decades. Further quantification will require more radiocarbon dates.

At Plaza H, MMB is generally a minor component of Terminal Classic contexts; in one analyzed unit, from the older portion of structure H-1, MMB comprises 4% of recovered sherds. Instead, serving vessels are largely comprised of the Belize Red group (red slipped, ash tempered vessels) alongside red slipped types from the calcite tempered Pine Ridge Carbonate ware (MMB is the black-slipped member). Notably, the four serving bowls included with the H-1 burial and are all red-slipped types from this ware (Aimers et al., 2019).

In general, the Terminal Classic peri-abandonment deposits show increased quantities of MMB (Awe et al., 2020a), and the deposit in Plaza H follows this trend. Around 13% of all sherds in levels identified with the H-1 peri-abandonment deposit are MMB. In the units adjacent to the structure, the densest part of the deposit with large sherds, the frequencies are above 20%. In short, at Plaza H, and across Cahal Pech, MMB use increased just at the end of archaeologically detectable activities (Aimers and Awe, 2020). Although more radiocarbon dates would be helpful, the difference in ^{14}C dates between the tomb and the

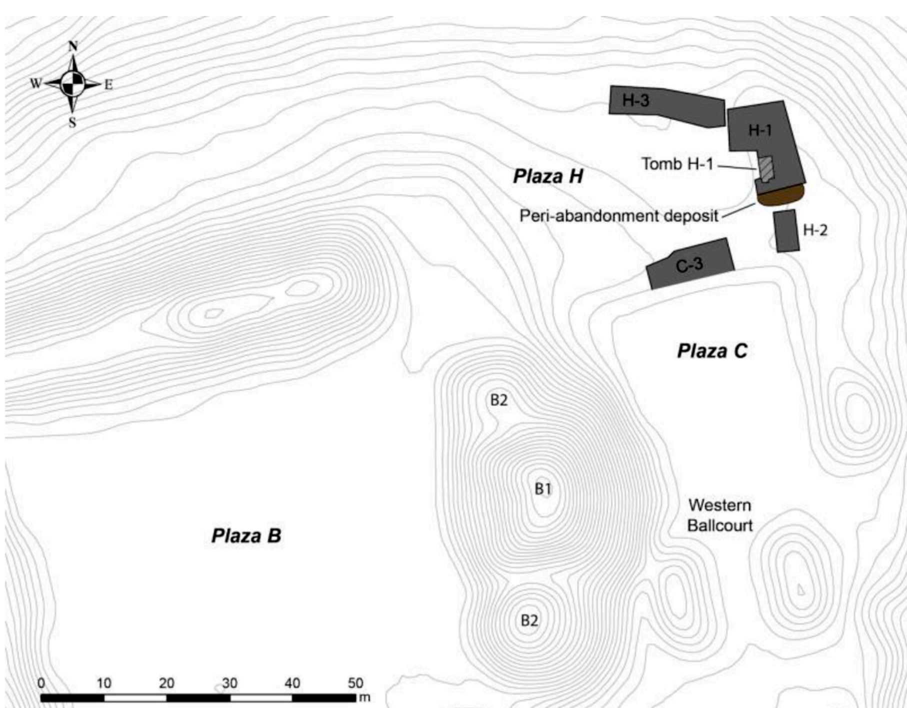

Fig. 2. The Plaza H location at the entrance to the primary Late Classic Plaza, B, Cahal Pech. Contour interval = 2 m.

peri-abandonment deposit suggests that this ceramic change occurred quickly during the ninth century and marks the closure of elite leadership living at the epicenter.

1.2. Research questions

Abrupt ceramic change holds interest to archaeologists. The observed increase in MMB frequency appears tied to a shifting economic and political landscape in the Terminal Classic. As outlined in 1.1.2, the tomb in H-1 appears to contain the last ruler buried at the Cahal Pech epicenter. The peri-abandonment deposit south of this tomb was created shortly after the residential use of Plaza H ceased. Thus, the deposit is a window into what occurred immediately after the failure of a Classic-style dynastic rulership at Cahal Pech, albeit one at a small scale. Further, MMB holds a unique place in the upper Belize Valley because of its firm connection with Xunantunich discussed in 1.1.1. This connection is both quantitative, with far more MMB found at Xunantunich than any other center in the Belize Valley, and qualitative, following LeCount's (2010) argument that these distinct serving vessels were a component of Xunantunich's social identity.

Viewed in this framework, the increased amount of MMB at the peri-abandonment deposit may be related to the breakdown of leadership at the Cahal Pech epicenter. To understand its significance, we sought to identify the source of the MMB sherds found there. Although many scenarios are possible, we concentrated on three hypotheses that relate to where production was centered. Hypothesis H_1 states that these vessels were produced at or nearby Xunantunich. If that is the case, the increase of MMB would physically relate to this competing center and its dominance in the Terminal Classic, and possibly carry the meanings that the type held at Xunantunich. H_2 states the type was produced near the Cahal Pech epicenter. Local ceramics would show continuity in nearby activities—and indicate that the abandonment of Cahal Pech as an elite residence was not immediately followed by the abandonment of close settlements. Of course, even if H_2 holds, the increase could still indicate emulation of Xunantunich, because social meaning and physical origins represent different kinds of interactions. Hypothesis H_3 states the type was made at diverse localities across the greater Belize Valley region, with no single recipe dominating. Such a change could indicate regional veneration at the H-1 burial, as represented by the peri-abandonment deposit, or disruption of nearby pottery-making communities. This hypothesis would align the abandonment of Plaza H with events across the Cahal Pech polity.

Definitive testing of these hypotheses requires provenance studies incorporating geological sourcing of raw materials or wasters from identified workshops (Waksman, 2017). However, as is typical in Maya utilitarian ceramic studies (Howie, 2005; Jordan et al., 2020), geographically identified sources are not available. Instead, we rely on the diversity and the spatial patterns of compositional groups defined in deposits of sherds discarded by users. Although the results cannot be as robust as having known ceramic production localities, it nevertheless delivers information to help infer the source—and by extension the underlying significance—of the ceramic shift.

2. Materials and methods

Both paste and slip were characterized to provide multiple lines of evidence. The 89 sherds that were examined for both slip and paste include samples from four localities: the Plaza H deposit in the Cahal Pech core ($n = 37$); a massive Terminal Classic ritual peri-abandonment deposit at Zopilote ($n = 18$), 750 m south of the Cahal Pech site core (Fox and Awe, 2017); a small sample collected at Tzutziiy K'in ($n = 10$), a Cahal Pech Late Preclassic to Terminal Classic elite residential group 1.8 km east of the core (Ebert et al., 2016, 2019); and a sample ($n = 24$) from the central plaza of Xunantunich recovered during conservation work at A-3, part of the eastern triadic structure (Zanotto and Awe, 2017). All the vessel forms were bowls. The sampling strategies differed; in the case of Tzutziiy K'in, we analyzed all recovered MMB sherds. With the larger assemblages, sampling priority was given to rim sherds with intact slip. Nonetheless, the slip is characteristically thin and patchy, a challenge for laser ablation.

The slip study was augmented by LA-ICP-MS analysis of 11 black slipped sherds from the San Jose Site, Orange Walk District, Belize, about 39 km north of Cahal Pech (Thompson, 1939). The sherds, curated at the Field Museum in Chicago, are Achote Black type, a member of the Peten Gloss ware. This is a ceramic type whose history, source, firing, temper, waxy slip, and likely uses all differ sharply from the prosaic, Belize Valley centered, MMB (Gifford, 1976). We included Achote Black samples in our analyses because of the shared black slip, whose general chemical variability in the Maya lowlands is poorly known. For the cluster analysis, these sherds provide an external reference collection, or outgroup, to assess the similarities and differences between the MMB sherds. Finally, their inclusion represented an opportunity to collaborate with the Field Museum's LA-ICP-MS laboratory, checking the viability of inter-laboratory studies, discussed further below. Intriguingly, Anna Shepard (1939) examined the San Jose collection in her first published technical study of Maya ceramics. With the San Jose sherds, the slip study includes 100 samples.

2.1. Slip characterization

The 89 sherds from Cahal Pech (Plaza H deposit), Xunantunich, Zopilote, and Tzutziiy K'in were prepared for LA-ICP-MS following routine procedures at the Archaeometry Lab at MURR. The 11 sherds from San Jose were analyzed by LA-ICP-MS at the Field Museum following a protocol similar to Halperin and Bishop (2016). Parameters for both analyses are detailed in Appendix A. Although not the focus of this study, an important methodological component was to evaluate data compatibility and reproducibility between instruments used at both laboratories to ensure accurate direct comparisons. Briefly, we used the same widely used reference materials (NIST-612 and NIST-610 issued by NIST; Brill B and Brill D issued by Corning), in-house quality controls (New Ohio Red Clay), consensus values (Pearce et al., 1997), and data reduction procedures (Dussubieux et al., 2009; Gratuze et al., 2001). Additionally, six duplicates of MMB sherds were analyzed by both instruments. For most key elements analyzed in the standard reference and quality control materials, concentration data were between 2 and 10%. For most key elements reported in the MMB duplicates, reported values were within 2–30%. Concentration data for 55 elements were reported; however, those with poor reproducibility due to the limits of detection (Ag, Au, In, Se, Tl), high within-sample variation (Cu, Y, Bi, Cs, Mo), variable volatilization or high ionization (P, S, Cl), or poor reproducibility (Co, Be, W) were deemed unreliable and excluded from the data set used for multivariate statistical interrogation. Appendix A provides details on the steps used in this data handling procedure.

Upon initial examination of the MMB slips from Cahal Pech and Xunantunich by LA-ICP-MS, seven samples were selected to further characterize their molecular and morphological compositions. They were selected based on their elemental concentration data (e.g. high vs low Fe, Mn, Ca) and site provenience (Cahal Pech or Xunantunich). SEM-EDS was used to characterize the pigment type and morphology (grain size, texture, homogeneity), and to create 2D elemental maps showing particle distribution on five of the sherds. XRD and Raman spectroscopy were used to identify dominant mineral phases in the slips and to determine if carbon used to color the slips could be attributed to a crystalline (graphite) or amorphous (charcoal, soot) mineral structure. Table 1 lists the specimens analyzed with these approaches. Appendix A describes the experimental parameters for each. Appendix B (.xls) provides spectral data for the XRD and Raman analyses.

2.2. Paste characterization

For the Upper Belize Valley MMB sherds ($n = 89$) in this analysis,

Table 1
List of specimens with slips analyzed by multiple methods. Slip compositional groups are described in 3.1.1.

Sample ID	Site	Compositional Group	SEM-EDS	XRD	Raman spectroscopy
MBV029	Cahal Pech	G1	X	X	
MBV031	Cahal Pech	G1			X
MBV045	Xunantunich	G3b	X		
MBV046	Xunantunich	G3b	X	X	X
MBV059	Xunantunich	G3b	X		
MBV062	Xunantunich	G3b		X	X
MBV064	Xunantunich	High Fe	X		

samples were analyzed by (NAA) using routine procedures for the analysis of pottery at the Archaeometry Lab at MURR (Glascock and Neff, 2003) and detailed in Appendix A. In short, a small piece (~2 cm^2) of each sherd was clipped and burred using a diamond drill bit to remove exterior surfaces on all sides and subsequently washed in deionized water. Each specimen was ground to a fine powder in an agate mortar and pestle. Two aliquots of the resulting powder were weighed into high-purity polyethylene or quartz vials used for irradiations. The samples were irradiated alongside NIST standard reference materials and the resulting gamma ray emissions were measured by hyper-pure germanium detectors. The analysis produced concentration data for 33 elements in all samples. The samples were subsequently compared to a regional database of over 25,000 previously analyzed ceramics (MURR Archaeometry Laboratory Database n.d.).

2.3. Results: slip composition

The elemental concentration data for all 100 slips are provided in Appendix B. To identify compositional groups in the slip recipes, we explored the distributions for multiple element pairs and through multivariate approaches, primarily principal components analysis (PCA), and hierarchical cluster analysis (HCA). Based on the PCA, Fig. 3 shows two scatterplots of (A) PC1 vs PC2 and (B) PC2 vs PC4. Fig. 4 shows two scatterplots of (A) hafnium vs calcium and (B) PC2 vs PC5. The PCA and element scatterplots reveal poor differentiation of site-specific groups within the dataset, with a significant overlap of all locations except for San Jose. The differentiation of San Jose in all plots was expected because it is outside the primary study area and represents a different type and ware.

2.3.1. Slip groups

The dendrogram in Fig. 5 illustrates the results of the HCA. In this test, five compositional groups (G1-G5) showed a tendency to cluster together, with two sub-groups (G3b, G4b), totaling seven clusters. This projection shows some site-specific differences, although differentiations are generally weak. Group 2 is comprised of San Jose samples. Groups 3a and 3b are similar to each other in composition, with both groups identified from Plaza H and Xunantunich samples. Groups 4a and 4b are primarily Zopilote and Tzutziiy K'in. Group 1 is distinct and dominated by samples from Plaza H, plus four from Zopilote. Samples denoted as "unassigned" are based on the PCA, yet some are reasonably consistent with clusters shown in the HCA. For instance, the Euclidean distance (ED) of MBV074, shown in Group 1, is low, suggesting that it is likely associated with that cluster. Conversely, unassigned samples MBV047 and MBV049 cluster with Group 5, but have high ED scores, indicating weak-positive clustering with Group 5. Except for San Jose, all of the compositional groupings represent samples from two or more sites, suggesting the predominant use of localized raw material use for slips with a small proportion of shared use of raw materials or the movement of finished vessels between localities.

2.3.2. Characterizing the slip groups

Table 2 (also in Appendix B) summarizes the average concentration, standard deviation (StDev), and relative standard deviation (RSD) for major oxides and trace elements for the slip groups. Except for Group 2 (all from San Jose), the groups show little variation in elemental chemistry, which is described below.

Selected samples listed in Table 1 were analyzed by SEM-EDS, XRD, and Raman spectroscopy. The mineral phases identified by XRD and Raman were associated with either the clay matrix used to produce the slip (or in part from the underlying ceramic), or the mineral colorant used to color the slip. All XRD and Raman spectra and peak pattern graphs are provided in Appendix B, and mineral phases are summarized in Table 3. In most or all samples, the mineral phases associated with the clay matrix included quartz, periclase, clinochlore, montmorillonite, sepiolite, and non-crystalline titanium-enriched aluminosilicates. Quartz (SiO_2) is a ubiquitous mineral in clays, occurring as a weathering product from the parent rock. Periclase is a common mineral in dolomitic limestone, a regionally ubiquitous bedrock. Clinochlore [$(Mg_5Fe)(AlSi_3)O_{10}(OH)_8$] is a mafic chlorite phyllosilicate mineral. Montmorillonite [$(Na,Ca)_{0.33}(Al,Mg)2(Si_4O_{10})(OH)_2{\cdot}nH_2O$] is a phyllosilicate mineral, one of the three most commonly identified in clays. Sepiolite [$Mg_4Si_6O_{15}(OH)_2{\cdot}6H_2O$] is a soft, magnesium silicate clay mineral. Calcite is the major temper material for MMB, identified by XRD in samples MBV029 (G1) and MBV046 (G3b).

The major mineral phases identified as colorants can be classified into two categories: carbon-based (graphite or charcoal), or oxides of iron and/or manganese (umber). Graphite is a distinct mineralization of carbon that is readily identifiable by XRD and Raman spectroscopy, whereas elemental carbon is non-stochiometric and is inferred to be probable soot or plant ash (van der Weerd et al., 2004). The term umber refers to a brown-black earth pigment made up of one or more mineral phases of iron and iron-manganese oxides. Umber is not a discrete mineral phase but is used as a category here for the identified minerals FeO, hematite, and Fe-Mn-Ox (disordered Fe-Mn-oxides).

2.3.2.1. Slip Group 1. Group 1, the largest compositional cluster, is dominated by samples from Plaza H with four from Zopilote. Samples MBV029 and MBV031 were selected for further characterization by SEM-EDS, XRD, and Raman spectroscopy. The average iron concentration for slips in Group 1 is 4.24 ± 1.41%, yet Fe-oxide phases were not readily identified by XRD, suggesting poorly crystalline iron oxide. Fig. 7A is an elemental map of MBV029 produced by SEM-EDS. The slip is a heterogeneous mixture, including discrete particles enriched in carbon (50–100 μm), calcium (likely calcite temper, 10–50 μm), and small particles (<5 μm) enriched in potassium, iron, phosphorus, and titanium. This slip recipe used a combination of poorly homogenized carbon and fine-grained iron oxides as mineral colorants.

2.3.2.2. Slip Group 2. This group is exclusively comprised of extra-local samples from San Jose. Group 2 is compositionally distinct from all other groups, and as notably high concentrations of CaO, B, Mo, Hf, and Pb, and depleted K, Cs, Tm, and Ni relative to other groups. Due to sampling restrictions, these could not be analyzed by additional techniques. However, they exhibited notably higher luster, opacity, and hue than MMB, and a more durable slip surface than the "fugitive" slip of MMB (Fig. 6). Intriguingly, although the slip from these Peten Gloss Ware cluster together, they also cluster with the majority of MMB slip groups (Fig. 5).

2.3.2.3. Slip Group 3. Slip Group 3 is the dominant group observed at Xunantunich (G3b), with a compositionally related sub-group (G3a), which includes specimens from both Xunantunich and Plaza H. Group 3a is depleted in Mg, but elevated in Sc, Cr, and Eu compared with other groups. Three samples from G3b were analyzed by SEM-EDS (MBV045, MBV046, MBV059) and one by XRD (MBV046). EDS maps in Fig. 7B–D illustrate these slips. MBV045 and MBV046 are similarly homogeneous in texture, with larger localized particles of carbon and calcium (5–20

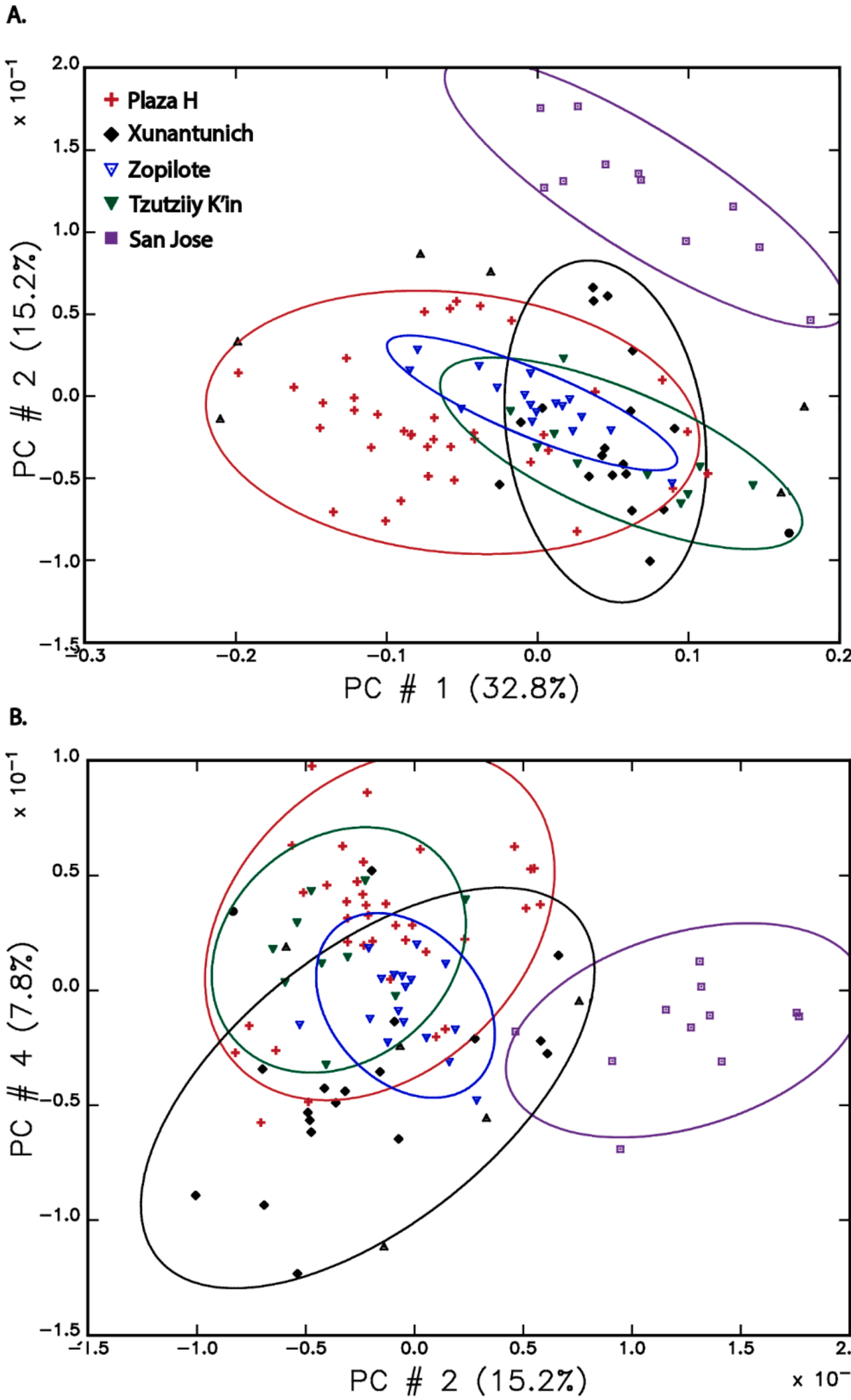

Fig. 3. PCA scatterplots of slip compositional data. (A) PC1 (32.8%) vs PC2 (15.2%). PC1 is positively driven by elements manganese, praseodymium, and cerium, while PC2 is positively driven by boron and lead. (B) PC2 (15.2%) vs PC4 (7.8%). PC4 is positively driven by barium, zinc, and nickel. Legend is shown in (A). Ellipses are drawn at the 90% confidence interval. Unassigned samples indicated by black triangles (▲).

μm), with fine-grained and more evenly distributed iron oxide particles. MBV059 shows a higher proportion of larger carbon particles. Interestingly, MBV046 and MBV062, from Xunantunich, were the only samples that potentially matched for the mineral graphite.

2.3.2.4. Slip Group 4. Slip Group 4 is largely comprised of samples from Tzutziiy K'in and Zopilote. There is a tendency for subgroups 4a and 4b to align with provenience, although not exclusively. Two specimens in Group 4b were from Plaza H. The iron concentrations for both groups average 4.25 ± 1.64% and 3.40 ± 1.98%, respectively. This is consistent with all other local groups, suggesting that FeO and carbon black were used to color the slips. Group 4a has notably higher Se and Co. No samples from these groups were available for analysis by additional methods, but they may warrant future investigation.

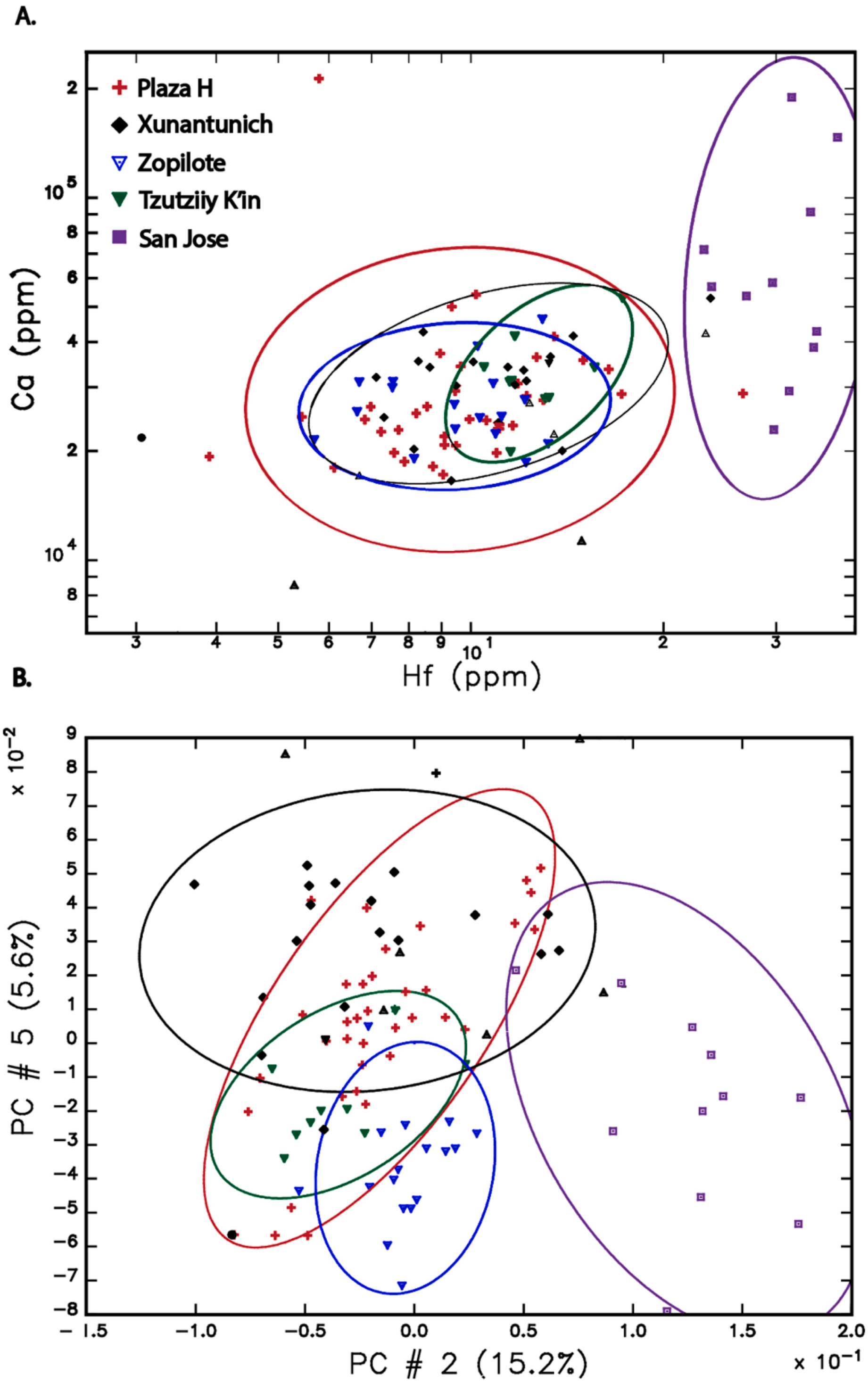

Fig. 4. Scatterplots of slip compositional data. (A) Hafnium versus cerium (ppm). (B) PC2 (15.2%) vs PC5 (5.6%). PC5 is positively driven by sodium, strontium, and magnesium. Legend is shown in (A). Ellipses are drawn at the 90% confidence interval. Unassigned samples indicated by black triangles (▲).

2.3.2.5. Slip Group 5. This group contains samples from Plaza H, Xunantunich, and Zopilote, including two samples from Xunantunich designated as "unassigned" by other multivariate statistical tests. Group 5 is characterized by lower K and Fe average concentrations. Overall, the specimens in Group 5 have limited affiliation with each other (indicated by ED scores in the HCA) and are considered outliers within the region.

Finally, outlier sample MBV064 from Xunantunich was not included in multivariate analyses (e.g., Fig. 5) because of concentrations uniquely high in Fe (17.7%) and Mn (0.5656%). MBV064 was analyzed by SEM-EDS (Fig. 7E), showing a dense and homogeneous distribution of fine-grained Fe-enriched particles with localized carbon particles (20–30 μm).

2.4. Results: paste compositional groups

A preliminary examination of the ceramic paste data was conducted with bivariate analysis for 89 Belize Valley MMB sherds. Through this visual examination, three macrogroups were identified, with some

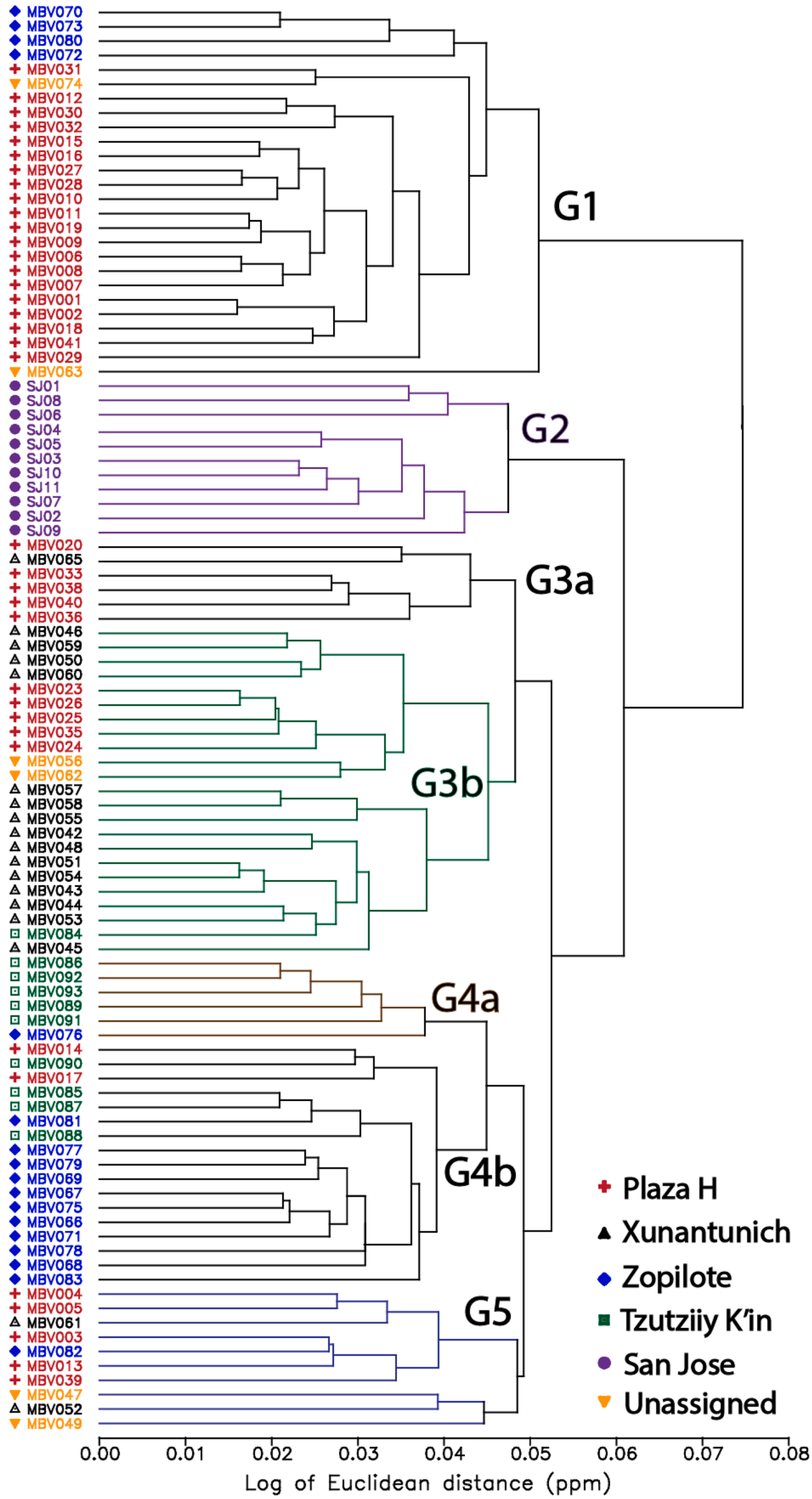

Fig. 5. Dendrogram showing the results of a hierarchical cluster analysis. Group clustering is designated by $^{\log}$ED scores between 0.04 and 0.06.

Table 2
Averages for Slip Compositional Groups. All concentrations listed in ppm unless otherwise noted (%).

	G1		n = 24	G2		n = 11	G3a		n = 6	G3b		n = 21	G4a		n = 7	G4b		n = 16	G5		n = 8
	AVG	StDev	RSD	AVG	StDev	RSD	AVG	StDev	RSD	AVG	StDev	RSD	AVG	StDev	RSD	AVG	StDev	RSD	AVG	StDev	RSD
Na2O (%)	0.1041	0.0408	39.20	0.3310	0.3592	108.52	0.1150	0.0660	57.40	0.3321	0.1404	42.26	0.1809	0.0817	45.15	0.1202	0.0271	22.58	0.2571	0.2641	102.70
MgO (%)	1.257	0.503	39.99	2.114	1.471	69.60	0.674	0.262	38.87	1.684	0.544	32.32	1.107	0.132	11.89	1.108	0.551	49.69	1.304	0.439	33.70
Al2O3 (%)	30.26	3.81	12.58	24.27	3.22	13.25	17.65	3.98	22.53	25.04	8.15	32.56	28.04	6.06	21.61	31.52	4.68	14.85	28.76	4.98	17.33
SiO2 (%)	54.35	4.90	9.02	58.55	5.77	9.85	65.71	7.91	12.03	59.69	6.93	11.61	55.70	2.05	3.68	54.90	5.61	10.22	58.04	4.33	7.47
K2O (%)	1.15	0.49	42.15	0.54	0.34	62.73	1.42	0.79	55.48	1.39	0.89	64.14	1.07	0.47	43.51	1.22	0.78	63.61	0.80	0.50	63.09
CaO (%)	4.46	5.43	121.85	10.19	7.22	70.82	3.53	1.32	37.48	4.58	1.27	27.82	4.72	1.53	32.44	3.87	0.81	20.83	5.09	1.31	25.76
Fe (%)	4.24	1.41	33.13	2.84	0.32	11.21	4.58	1.52	33.11	3.37	0.71	20.98	4.25	1.64	38.52	3.40	1.98	58.16	2.69	0.63	23.55
Li	98.51	22.20	22.54	93.69	64.11	68.42	106.42	35.59	33.44	68.89	26.18	38.00	144.99	52.47	36.19	145.87	32.15	22.04	106.58	47.28	44.36
Be	4.88	1.32	27.00	2.56	0.95	36.94	4.66	1.61	34.61	5.60	2.40	42.94	10.54	2.48	23.57	6.18	1.86	30.15	7.52	1.97	26.23
B	28.38	11.13	39.20	268.55	194.54	72.44	64.99	26.38	40.58	43.40	17.63	40.63	39.86	23.15	58.07	48.43	12.47	25.74	58.40	24.32	41.64
P	447.73	151.52	33.84	2239.79	1341.30	59.89	330.34	246.08	74.49	500.66	286.94	57.31	777.88	335.35	43.11	745.68	530.49	71.14	623.57	375.48	60.21
S	580.10	271.88	46.87	–	–	–	1481.78	1531.40	103.35	590.69	480.18	81.29	955.34	645.48	67.57	774.43	550.53	71.09	507.76	355.72	70.06
Cl	888.59	746.04	83.96	–	–	–	291.63	158.99	54.52	835.73	543.68	65.05	747.86	426.45	57.02	683.17	384.69	56.31	497.60	867.91	174.42
Sc	17.62	4.06	23.02	12.00	1.96	16.35	51.01	9.68	18.98	20.28	7.30	36.00	22.80	2.08	9.13	21.28	5.35	25.13	17.27	2.79	16.14
Ti	6548.58	983.31	15.02	5471.96	903.28	16.51	6262.69	1331.61	21.26	5640.39	1034.81	18.35	7705.41	1604.14	20.82	9200.94	4405.01	47.88	6459.75	1759.31	27.23
V	77.51	20.84	26.88	105.19	22.33	21.23	69.24	24.43	35.28	72.76	16.27	22.36	89.22	19.96	22.37	104.57	33.44	31.97	75.33	11.87	15.76
Cr	107.54	19.29	17.94	143.09	37.09	25.92	245.46	56.20	22.90	95.77	30.83	32.19	102.30	39.99	39.09	115.26	25.05	21.74	79.61	12.57	15.79
Mn	152.37	95.67	62.79	351.27	315.61	89.85	120.80	102.23	84.62	490.09	464.54	94.79	647.87	436.23	67.33	308.77	347.50	112.54	236.34	239.84	101.48
Co	8.13	6.76	83.20	15.81	11.35	71.77	14.84	4.32	29.15	11.60	7.70	66.40	46.51	30.39	65.33	16.28	10.50	64.47	9.06	4.89	53.94
Ni	79.75	32.85	41.19	32.32	7.22	22.33	81.58	17.08	20.94	59.76	26.97	45.13	92.26	18.70	20.27	74.92	33.99	45.37	88.16	38.87	44.10
Cu	223.57	102.05	45.65	110.33	77.73	70.45	265.09	94.52	35.65	248.32	182.45	73.47	263.07	127.47	48.45	197.97	156.27	78.94	298.62	110.39	36.97
Zn	444.23	142.88	32.16	153.82	67.33	43.77	560.36	277.89	49.59	360.15	182.40	50.65	500.87	175.33	35.01	432.05	192.36	44.52	718.14	392.87	54.71
As	15.17	7.53	49.63	18.04	7.20	39.91	10.97	2.86	26.11	12.22	7.12	58.30	43.59	21.48	49.28	33.38	11.12	33.32	28.40	16.32	57.47
Se	1455.98	726.62	49.91	–	–	–	566.43	620.94	109.62	488.40	652.03	133.50	1574.42	903.88	57.41	949.63	528.84	55.69	210.67	284.42	135.01
Rb	223.23	88.23	39.52	149.76	52.31	34.93	212.02	157.18	74.14	156.15	33.92	21.72	178.51	73.45	41.15	216.55	130.09	60.07	264.37	158.87	60.10
Sr	47.82	14.37	30.06	79.80	42.07	52.72	56.57	36.50	64.52	111.57	29.49	26.43	86.42	24.02	27.79	64.19	17.14	26.71	89.81	35.82	39.89
Y	11.82	3.00	25.36	15.12	9.65	63.86	14.21	6.55	46.11	20.76	5.42	26.13	31.99	10.91	34.10	21.33	6.34	29.72	23.17	6.15	26.54
Zr	194.06	40.52	20.88	322.08	19.37	6.01	166.05	69.86	42.07	279.42	76.45	27.36	292.85	60.87	20.78	249.68	68.24	27.33	331.64	36.08	10.88
Nb	22.97	5.13	22.32	38.31	5.69	14.85	24.19	7.03	29.08	20.52	4.83	23.53	29.52	7.75	26.26	31.04	10.12	32.60	29.21	8.79	30.10
Mo	0.94	0.41	43.88	8.09	15.19	187.80	1.88	0.45	24.11	1.90	0.91	47.78	1.73	1.24	71.45	1.28	0.72	56.24	2.79	1.29	46.10
Ag	0.29	0.15	52.09	0.63	0.43	67.94	0.87	0.53	60.64	0.43	0.21	48.63	0.35	0.17	48.70	0.44	0.20	44.87	0.59	0.28	48.50
Sn	9.27	3.98	42.95	10.53	2.70	25.65	8.61	2.90	33.70	8.45	4.85	57.40	7.47	2.48	33.13	7.42	2.77	37.30	12.70	8.65	68.11
Sb	2.11	0.75	35.68	5.23	1.23	23.57	1.63	0.59	35.83	2.74	0.84	30.71	2.81	0.98	34.86	2.58	1.12	43.29	3.66	1.21	33.21
Cs	28.21	16.93	60.03	5.13	3.10	60.42	22.62	16.47	72.83	12.89	6.16	47.78	15.63	5.79	37.04	21.67	14.11	65.09	19.31	10.94	56.68
Ba	1341.36	472.38	35.22	947.36	433.02	45.71	926.37	196.47	21.21	1147.97	834.59	72.70	922.12	184.97	20.06	1014.29	746.41	73.59	1637.25	868.16	53.03
La	19.60	7.70	39.29	52.86	41.00	77.57	22.46	11.74	52.25	50.50	21.85	43.27	71.86	28.35	39.46	37.86	14.69	38.82	34.65	19.02	54.89
Ce	40.19	16.34	40.67	199.25	145.32	72.93	51.24	40.58	79.20	66.81	33.54	50.20	165.92	83.33	50.22	131.30	96.64	73.60	60.57	20.62	34.04
Pr	4.44	1.80	40.60	16.73	12.33	73.70	5.03	2.54	50.40	10.03	3.38	33.68	18.95	5.02	26.49	10.65	5.07	47.60	11.67	3.63	31.16
Nd	19.51	8.14	41.70	79.46	59.54	74.93	25.33	16.23	64.07	41.13	14.45	35.15	69.28	16.73	24.16	40.68	13.56	33.34	29.97	8.07	26.91
Sm	4.67	1.91	40.89	13.07	8.83	67.57	5.97	3.19	53.44	9.25	2.96	32.06	16.09	3.33	20.70	8.16	2.82	34.55	10.29	2.90	28.12
Eu	1.15	0.35	30.44	1.47	0.87	59.23	17.19	5.12	29.77	2.58	2.83	109.55	2.74	0.43	15.59	1.78	0.58	32.34	2.30	1.17	51.01
Gd	9.53	4.56	47.81	9.39	5.75	61.20	9.17	3.23	35.24	10.83	3.73	34.48	12.03	2.42	20.11	9.89	4.17	42.13	18.23	5.41	29.66
Tb	1.02	0.39	37.83	1.80	1.01	56.27	2.45	1.23	50.38	2.15	1.25	57.95	2.76	0.39	14.02	1.59	0.44	27.64	3.62	3.11	85.89
Dy	5.02	1.79	35.71	20.70	10.39	50.19	7.65	3.55	46.36	10.66	3.24	30.43	17.88	3.54	19.82	9.18	2.42	26.36	17.46	4.96	28.40
Ho	1.22	0.37	30.09	2.39	1.12	46.95	1.94	1.80	92.97	2.19	0.47	21.34	3.35	1.09	32.71	2.13	0.61	28.46	5.69	3.10	54.59
Er	3.40	1.18	34.81	7.94	3.50	44.06	4.96	2.63	52.99	6.01	2.07	34.40	9.57	2.16	22.58	4.80	1.12	23.30	16.04	6.72	41.88
Tm	0.84	0.37	44.51	0.22	0.09	42.32	1.11	0.69	62.13	0.81	0.62	76.73	1.81	0.46	25.54	1.08	0.37	34.40	0.94	0.56	59.21
Yb	4.19	1.30	31.01	4.85	1.88	38.80	4.69	2.46	52.56	4.95	2.36	47.74	10.48	2.81	26.84	6.54	3.07	46.94	13.82	7.58	54.90
Lu	0.56	0.18	31.98	1.24	0.49	39.21	0.57	0.40	70.09	0.84	0.26	30.81	1.27	0.48	37.76	0.93	0.34	37.23	3.83	2.96	77.18
Hf	8.91	1.96	21.96	30.61	4.55	14.87	9.13	3.70	40.55	10.29	1.80	17.54	12.21	3.25	26.63	10.82	2.72	25.12	16.30	6.28	38.55
Ta	2.17	0.57	26.26	4.33	0.97	22.53	3.20	1.92	59.89	1.90	0.59	30.89	3.10	1.18	37.88	2.80	0.78	27.76	3.62	2.13	58.73
W	3.32	1.30	39.22	7.99	1.73	21.69	3.67	1.02	27.91	3.27	1.25	38.34	5.55	4.08	73.56	3.79	1.00	26.45	5.87	2.72	46.29
Au	0.05	0.05	97.15	–	–	–	0.10	0.08	78.24	0.14	0.14	98.97	0.08	0.04	48.47	0.05	0.03	58.21	0.65	1.11	169.38
Tl	10.43	3.76	36.08	–	–	–	12.79	5.93	46.39	6.39	1.81	28.32	12.28	3.86	31.44	9.94	4.22	42.47	15.87	7.96	50.16

(*continued on next page*)

Table 2 (*continued*)

	G1		n = 24	G2		n = 11	G3a		n = 6	G3b		n = 21	G4a		n = 7	G4b		n = 16	G5		n = 8
	AVG	StDev	RSD	AVG	StDev	RSD	AVG	StDev	RSD	AVG	StDev	RSD	AVG	StDev	RSD	AVG	StDev	RSD	AVG	StDev	RSD
Pb	43.22	15.54	35.96	191.49	69.21	36.14	40.95	17.04	41.62	49.82	19.04	38.22	80.44	36.59	45.48	55.60	18.14	32.63	61.11	13.09	21.42
Bi	5.28	4.11	77.70	9.26	3.76	40.66	1.45	0.71	48.80	2.79	3.38	120.85	3.65	4.79	131.19	1.71	1.05	61.50	10.63	9.35	87.95
Th	19.60	6.24	31.84	58.79	11.98	20.38	23.45	7.05	30.06	23.88	5.60	23.45	25.57	4.11	16.09	25.45	9.11	35.78	36.81	11.91	32.35
U	2.02	0.89	44.09	3.78	1.28	33.84	1.97	0.64	32.50	1.86	0.63	34.02	2.67	0.88	33.00	3.19	1.00	31.35	3.76	1.40	37.26

internal sub-groupings. Fig. 8 is a scatterplot showing the distribution of sub-groupings and the three unassigned outliers. MBV076 (Zopilote) shows general characteristics similar to macrogroup 2 (G2), yet plots away from the cluster. This could be considered a G2 outlier. Sample MBV060 (Xunantunich) exhibits a similar pattern, falling along the trendline for G3, yet plots away from the main cluster. MBV090 (Tzutziiy K'in) also exhibits this trend with G1 and it is considered a G1 outlier.

As seen in Table 4, paste sorts differentially between localities, suggesting a link between the deposits and the paste characteristics. The Plaza H deposit consists of only G3 ceramics, even though it is the largest sample, with two sub-groups dominating. G3 is also important at Xunantunich, but Xunantunich is the only site with all three groups represented. Zopilote is unusually variable, especially considering the sample size. Tzutziiy K'in has a single subgroup, G1-B, dominating, making it the locality with the most distinct and homogeneous paste recipe.

NAA characterization of the paste allows broader comparisons with previously analyzed samples at MURR. Specifically, Ebert et al. (2019) conducted NAA on 192 sherds recovered from Cahal Pech site core, Zopilote, and Tzutziiy K'in, pottery manufactured during the Preclassic period (1000 BCE–300 CE) up to 1800 years before the manufacture of the MMB sherds considered here. In that study, seven distinct compositional groups were identified, which were used to compare with the present data set. The Group G sherds reported in the previous study (n = 45), dating from the start of the Jenny Creek Phase (900 BCE), closely match the G3 group documented here, a fit that is striking when the current study is projected onto the Preclassic groupings (Fig. 9). Ebert et al. (2019), after comparing their groups against all 25,000 Mesoamerican sample sherds in the MURR database, concluded that the Cahal Pech area Preclassic ceramics were locally produced. Combining these studies shows a tremendous continuity between the Preclassic G and the Terminal Classic G3 macrogroup. MMB pottery found in Plaza H originated in the Cahal Pech area.

3. Discussion

We characterized MMB sherds from a peri-abandonment deposit at Plaza H, Cahal Pech, linked to one of the last identifiable organized Terminal Classic activities at the epicenter. Lacking source evidence from ceramic workshops, we compared the assemblage with other localities in the Cahal Pech polity, and, most critically, with the Xunantunich epicenter. Both slip and paste characterization show significant differences between the Plaza H and the Xunantunich samples, with Xunantunich being more diverse. However, 67% of Xunantunich and all of Plaza H samples employ the long-standing paste composition macrogroup 3. Paste, therefore, does not distinguish between the localities as clearly as the slip groups, which overlap less and, as demonstrated in the auxiliary studies in 3.1.2, rely on different colorants and recipes. Samples from Zopilote and Tzutziiy K'in in the greater Cahal Pech polity demonstrate that diverse sources of MMB are distributed in a nonrandom pattern within the Cahal Pech polity.

To further illustrate and refine these observations, the intersection of slip and paste recipes for each sherd was examined (Table 5). Out of the 120 combinations of slip/paste subgroups possible, 31% occur, with 20 of the 37 observed combinations represented by a single sherd. Although not all paste groups have corelating slip groups, correlations are evident in the highlighted cells of Table 5, comprising about half the sampled sherds. Tzutziiy K'in shows a strong pattern of G-1b paste with G-4 slip co-occurrence (80% of 10). In contrast, Zopilote has the greatest number of slip-paste combinations (13) even with its modest sample size (18). The large Plaza H sample is dominated by two major variants: the G3 macrogroup paste with either G1 slip (54% of the sample) or G3 slip (24% of the sample). The combinations appear to be largely specific to Plaza H and can be considered the local recipe. Intriguingly, the combination of G3-C paste and G3b slip is shared at both Plaza H (13%) and

Table 3
List of mineral phases identified by XRD and Raman spectroscopy. Carbon was verified by both XRD and Raman in MBV031 and MBV046. Graphite was a weak positive match in MBV062. Hematite was a weak positive match in MBV046.

	MBV029	MBV031	MBV046	MBV062
Clay Phases				
Quartz	X		X	X
Calcite	X		X	X
Montmorillonite	X			
Clinochlore	X			
Sepiolite			X	X
Al-Ti (disordered)			X	X
Periclase	X			X
Mineral Colorant Phases				
Carbon (charcoal)	X	X	X	X
Graphite			X	X
FeO			X	
Hematite			X	
Fe-Mn-Ox (disordered)				X

Xunantunich (17%). This specific recipe at both centers shows a connection overlaid on the significant differences in MMB composition seen when the samples are compared as a whole. More generally, the Xunantunich sample is diverse (although less so than Zopilote), supporting earlier research that production there was dispersed and variable (Garcia, 2008; LeCount, 2010).

Table 5 provides the final data set to evaluate the three hypotheses found in Section 1.2. The production of MMB ceramics from the peri-abandonment deposit in Plaza H appears to be largely local, fitting hypothesis H_2. "Local" is a relative term, but the distinctiveness of the Plaza H compositional groups compared with Tzutziiy K'in and Zopilote suggests that ceramic production of MMB was highly localized and that production within the polity was dispersed. Although we lack workshop data that would verify this inference, a continuation of ceramic manufacture near the Cahal Pech epicenter is inferred. Such production would indicate that the cessation of elite occupation at Plaza H did not necessarily mark the simultaneous collapse of local communities. The H_2 hypothesis of local production of the MMB recovered in Plaza H was previously supported by Johannesen (2018), who compared vessel form and the temper for many of the same Xunantunich and Plaza H sherds examined here. That study employed microphotography and thin sections to demonstrated temper differences between the localities. Johannesen (2018) also observed that the bowl lip forms at Plaza H do not fit the Xunantunich microseriation: Plaza H retained the Late Classic microstyle found at Xunantunich.

Interestingly, it is the samples from Zopilote, about 1 km south of the Cahal Pech epicenter, that fits hypothesis H_3: that is, diverse nonlocal sources. Zopilote, linked to the Cahal Pech epicenter by a causeway, represents a unique context: a massive peri-abandonment deposit of smashed Terminal Classic pottery at an elite Late Classic tomb, possibly that of a ruler (Awe, 2013; Fox and Awe, 2017). The diversity of MMB ceramics at Zopilote suggests that ceremonial activities may have attracted distant participants and their pottery. Both Zopilote and Plaza H samples derive from peri-abandonment deposits located adjacent to elite tombs of potential Cahal Pech rulers, yet the differences in diversity (along with differences in the magnitude of the deposits) suggests dissimilar scales of ritual participation. In contrast, the small domestic Tzutziiy K'in assemblage fits the H_2 local supplier model. The Tzutziiy K'in sherds come from the residence of an intermediary elite family somewhat distant from the epicenter. The relative uniformity and distinctiveness of the ceramics from this locality suggest that a single local supplier produced most of the MMB found there.

The overlapping patterns of somewhat distinct paste and slip groups, which partially distinguish between localities, suggests that local production and consumption was the most common pattern. Broadly, the results fit closely previous studies of Maya serving and utility vessels discussed in Section 1. Specifically, the results strengthen the "constellation of practice" behavioral model of ceramic production inferred by Jordan et al. (2020) for the Belize Valley. They envision multiple discrete communities that manufactured ceramics, whose product is partially distinguishable on technological grounds, but share general production and style frameworks. Notably, Jordan et al. (2020) base this

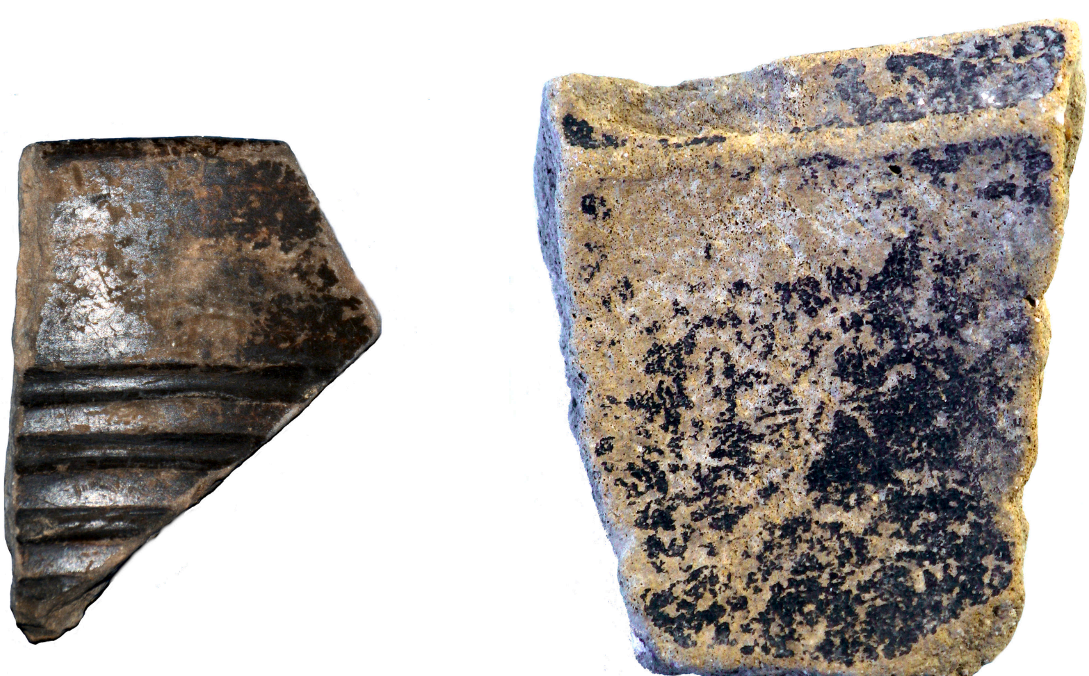

Fig. 6. Exterior, Achote Black, Cubeta Incised Variety, from San Jose (left, SJ10) and interior MMB bowl sherd (right, MBV074); sherd on left, 4 cm.

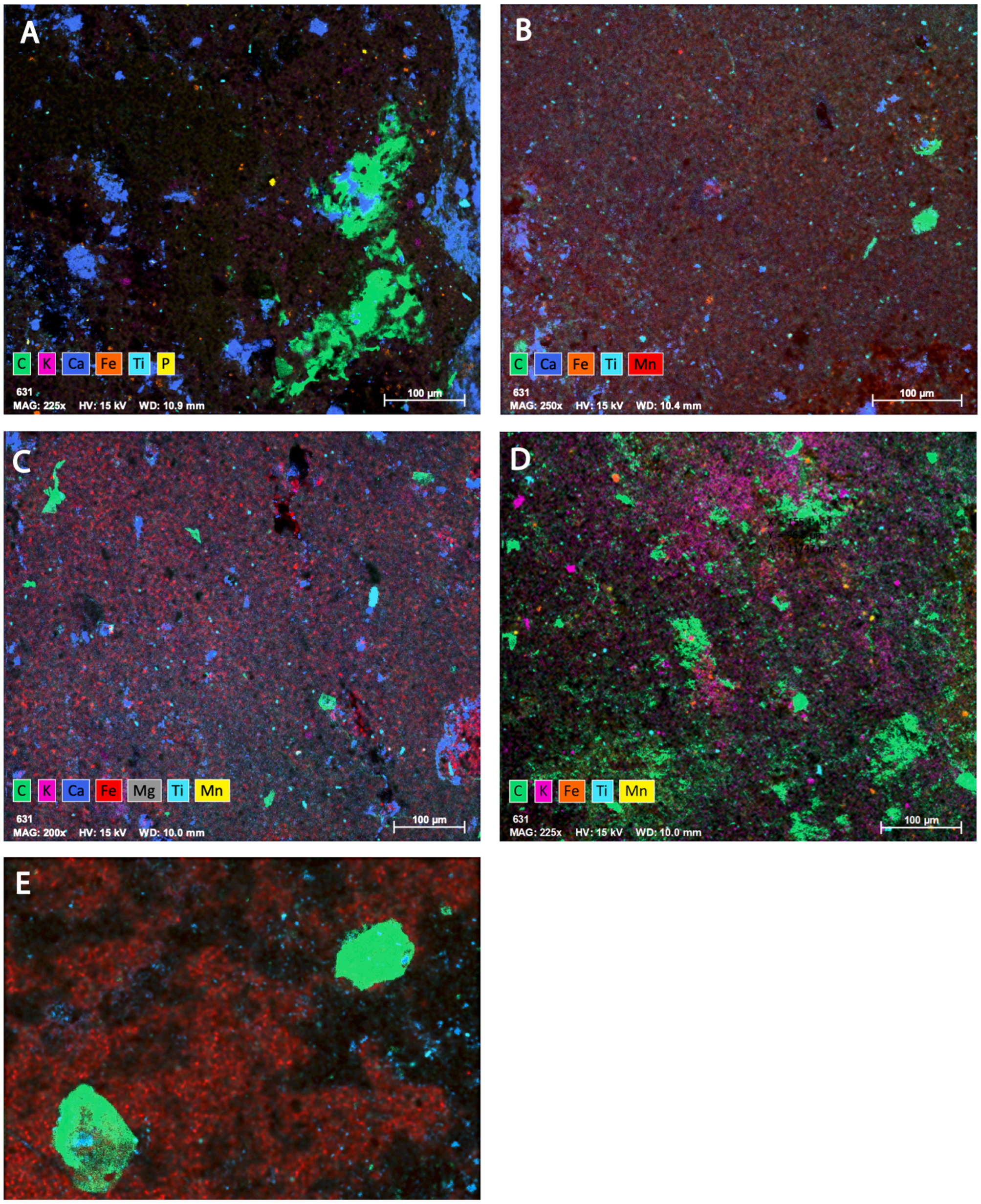

Fig. 7. Hyperspectral EDS maps for selected samples. (A) MBV029 from slip Group 1. Regions in black are enriched in Al-Si (clays). (B-C) MBV045 and MBV046 from Group 3b. (D) MBV059 from Group 3b. (E) MBV064 outlier with high iron and manganese. Scale bar in A-D = 100 μm; Scale bar in E = 30 μm.

conclusion on other methods and data not used in this study: thin section and macroscopic observations of unslipped pottery from Baking Pot (located in Fig. 1).

4. Conclusions

This study establishes critical parameters for interpreting the spike in MMB ceramics around the time Cahal Pech ceased serving a habitation function. Initially, our explanations focused on the linkage of MMB with Xunantunich, echoing traditional archaeological narratives connecting ceramic style shifts with external "centers" that generate change. Yet, Cahal Pech's MMB derives from more localized ceramic production, ongoing before MMB became a common ceramic type. The type was produced with a ceramic paste macrogroup that is part of an 1800 year production tradition in the Cahal Pech region. The NAA evidence for continuity at Cahal Pech is strong, and it fits continuity shown in other Maya regions (notably, Lamanai, in northeast Belize; Howie, 2005:357). Maya potters could maintain the long-term stability of paste recipes while adapting to trends in vessel form, surface treatment, and decoration across the millennia.

Nonetheless, the increase in MMB vessels is novel for Cahal Pech, which calls for an explanation. Increased amounts of MMB *could* reflect a deliberate emulation of a powerful neighbor, and *might* even reflect the adoption of the values linked to the ceramic type by LeCount's (2010) interpretation for Xunantunich. However, neither idea is supported by the current evidence. Cahal Pech potters did not closely mimic the bowl lip forms from Xunantunich, suggesting they were unconcerned with replicating contemporary vessels. Further, LeCount's model hinges on daily practice and experience as the means to build shared values, which does not fit the observed rapid ceramic change. It is more reasonable to assume that Cahal Pech potters worked from a standing parallel tradition. More plausibly, the increased quantities of this local variant of

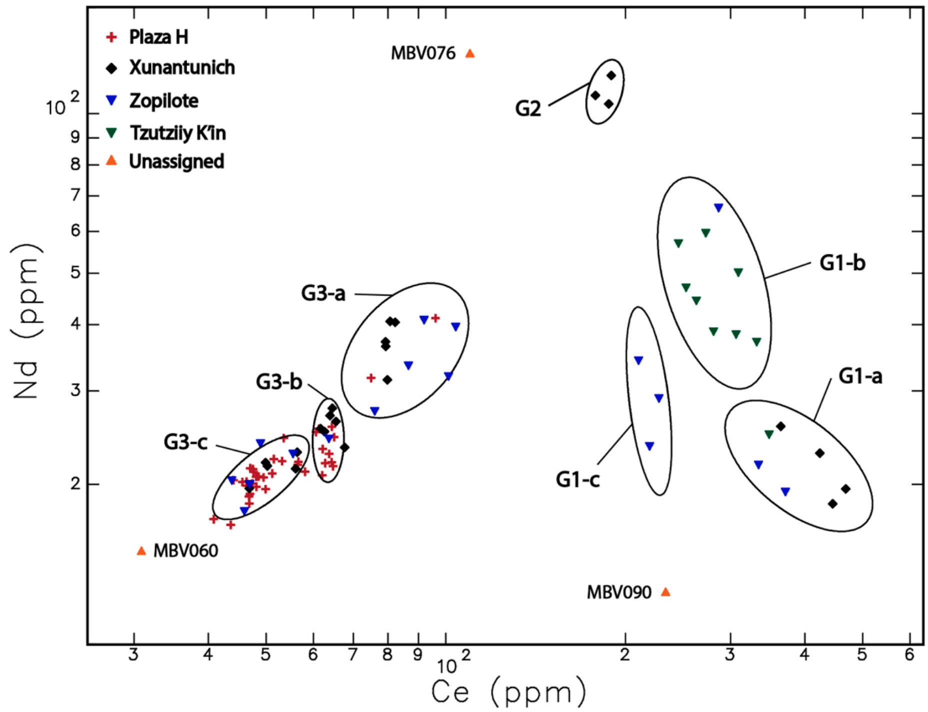

Fig.8. Scatterplot of cerium versus neodymium, showing the distribution of macro- and sub-groups for MMB-series samples, and three unassigned outliers (labeled). Ellipses are drawn at 90% confidence.

Table 4
Distribution of paste groups by location.

	G1-A	G1-B	G1-C	G2	G3-A	G3-B	G3-C	UNAS	TOTAL
Plaza H	–	–	–	–	2	10	25	–	37
Xunantunich	4	–	–	3	5	6	5	1	24
Tzutziiy K'in	1	8	–	–	–	–	–	1	10
Zopilote	2	1	3	–	5	1	5	1	18
Total	***7***	***9***	***3***	***3***	***12***	***17***	***35***	***3***	***89***

MMB relates to the dynamics and availability of other serving vessel types as the events of the Terminal Classic altered trade and interaction. Such changes may have favored the local products of potters over those that may have been imported from other centers, such as Belize Red. Broader sourcing of Terminal Classic serving vessels at Plaza H would further clarify the roots of this ceramic shift.

Our unique examination of both paste and slip composition in this study highlights the potential for slip recipes as indicators of communities of practices, as well as providing data about slip ingredients as indicators of long-distance exchange. From ethnoarchaeological data, Arnold (1985) established that traditional potters frequently acquire slip and paint ingredients from far greater distances than the clay body. For example, Thompson's (1958) study of contemporary Maya potters of the northern Yucatan identified "iron-manganese concretions," found in swampy areas, as the source of black paint. Thompson establishes that these concretions were difficult to obtain in his study area, and cites earlier work that the material sometimes came from sources over a 100 km away. Such concretions could be a source for some elements found in slip recipes, especially for MBV064. Arnold (1985) speculated that because paints and slips are frequently transported great distances, archaeological trade networks akin to obsidian exchange might be found.

The current study modifies this claim by showing that slip recipes also can be specific and localized, modifying some older views. Shepard (1956) had suggested that Maya black slip might have relied on a single recipe, and our analysis of the San Jose site Achote Black sherds confirms that fine ceramics from a single site can have homogenous slip composition, helping to situate Shepard's view. But the lesson of our broader study is that the Maya had multiple means to achieve a black slip, and these recipes vary considerably.

Three sherds from Xunantunich are particularly interesting in documenting slip variation: MBV064 (omitted from the statistical analysis), discussed above, with uniquely high concentrations of Fe and Mn, and MBV046 and MBV062, with evidence of graphite. Because our LA-ICP-MS procedure does not readily quantify carbon, the extent of graphite use at Xunantunich is presently unknown, but these three sherds indicate that mineral colorants were critical in some slip recipes. These mineral colorants support Arnold's inference (1985) that raw materials for slip may be an underutilized item for examining long-distance exchange. Specifically, the graphite employed at Xunantunich suggests a future avenue of study. The only documented graphite source in the region is located about 40 km away from the Belize Valley in the foothills of the Cockscomb Range (Miller, 1915). This material might be a candidate to identify exchange networks, assuming distinct trace elements are identified from source samples.

In closing, this study happened to incorporate ceramics from the center where Anna Shepard (1939) conducted the first technological ceramic study for the Maya region. While not part of the original

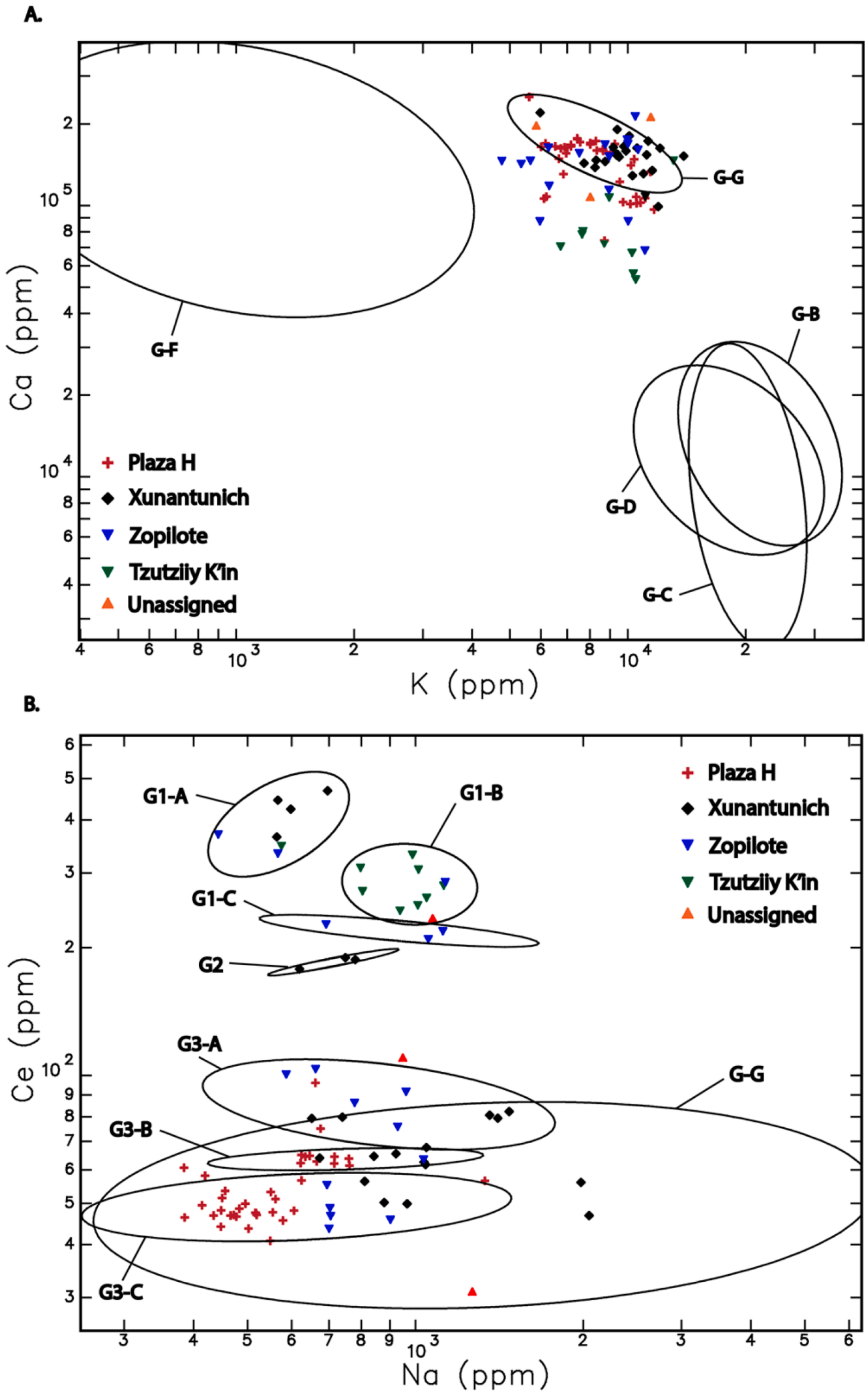

Fig. 9. Comparison to compositional reference groups reported in Ebert et al 2019. Ellipses are drawn at 90% confidence and represent compositional reference groups, while sample icons represent new data points. (A): Scatterplot of K versus Ca. Samples from the present study do not correlate with Ebert's reference groups B, C, D, or F. (B) Scatterplot of Na versus Ce. Samples from paste Group 3 of the present study are strong matches for Ebert's Group G. Samples from paste Groups 1 and 2 show elevated cerium, but are still highly compatible with Ebert Group G when compared with other compositional groups.

research design, this coincidence is a reminder that ceramic research has a long history in the region, but has yet to reach full potential. The present study is one of the first to combine the geochemical characterization of ceramic pastes with slips from the Maya lowlands. Using these techniques for a fine-grained focus on everyday Maya ceramics from a specific context illustrates how social history, economic organization, and networks can be monitored by moving away from typological pottery analysis and towards the identification of specific compositional recipes.

CRediT authorship contribution statement

John E. Douglas: Conceptualization, Writing - original draft, Funding acquisition. **Brandi L. MacDonald:** Methodology, Investigation, Formal analysis, Writing - original draft. **Claire E. Ebert:** Resources, Visualization. **Jaime J. Awe:** Resources. **Laure Dussubieux:** Investigation, Resources. **Catherine E. Klesner:** Investigation.

Table 5
Distribution of paste/slip combinations (rows; slip groups in parentheses) by locality (columns). The same-colored cells highlight higher-frequency combinations that might represent favored paste-slip combinations.

Paste+Slip Group	Plaza H	Tzutziiy K'in	Xunantunich	Zopilote	Total
G1-A (G3a)			1		1
G1-A (G3b)		1			1
G1-A (G4b)				1	1
G1-A (G5)				1	1
G1-A (UNAS)			3		3
G1-B (G4a)		5			5
G1-B (G4b)		3		1	4
G1-C (G1)				1	1
G1-C (G4b)				2	2
G2 (G3b)			3		3
G3-A (G1)	1			1	2
G3-A (G3b)			3		3
G3-A (G4b)	1			4	5
G3-A (G5)			2		2
G3-B (G1)	5				5
G3-B (G3a)	1				1
G3-B (G3b)			4		4
G3-B (G4b)				1	1
G3-B (G5)	4				4
G3-B (UNAS)			2		2
G3-C (G1)	14			2	16
G3-C (G3a)	4				4
G3-C (G3b)	5		4		9
G3-C (G4a)				1	1
G3-C (G4b)	1			1	2
G3-C (G5)	1				1
G3-C (UNAS)			1	1	2
UNAS (G3b)			1		1
UNAS (G4a)				1	1
UNAS (G4b)		1			1
Total	**37**	**10**	**24**	**18**	**89**

Acknowledgments

This research is part of the Belize Valley Archaeological Reconnaissance (BVAR) Project, directed by Jaime Awe, Julie Hoggarth, and Claire Ebert, and supported by the Belize Institute of Archaeology, including Director John Morris. The excavations of the Plaza H peri-abandonment deposit were conducted by field school students from the University of Montana. Support for some analyses was provided by the UM Humanities Institute, College of Humanities and Sciences, and the UM Sponsored Research Small Grant Program. Other research was supported by the NSF-1912776 grant to the Archaeometry Laboratory. We thank Julie Hoggarth for providing the ^{14}C dates for Plaza H. We thank David Stalla (University of Missouri Electron Microscopy Core) for assistance with SEM-EDS, and Stephen Kelley (University of Missouri, Chemistry Department) for assistance with XRD. We thank Michael D. Glascock for assistance with NAA. Finally, we thank the anonymous reviewers for their helpful insights.

Appendix A. Supplementary data

Supplementary data to this article can be found online at https://doi.org/10.1016/j.jasrep.2020.102666.

References

Aimers, J.J., Awe, J.J., 2020. The long goodbye: problematic pottery and pilgrimage at Cahal Pech, Belize. Ancient Mesoam 31, 151–160. https://doi.org/10.1017/S0956536119000191.

Aimers, J.J., Awe, J.J., LeCount, L.J., 2019. A contextual analysis of Terminal Classic vessels from Cahal Pech, Belize. Res. Rep. Belizean Archaeo. 16, 133–141.

Arnold, D.E., 1985. Ceramic Theory and Cultural Process. Cambridge University Press, New York.

Awe, J.J., 2013. Journey on the Cahal Pech time machine: An archaeological reconstruction of the dynastic sequence at a Belize Valley Maya polity. Res. Rep. in Belizean Archaeo. 10, 33–50.

Awe, J.J., Ebert, C.E., Hoggarth, J.A., Aimers, J.J., Helmke, C., Douglas, J., Stemp, W.J., 2020a. The last hurrah: Examining the nature of peri-abandonment deposits and activities at Cahal Pech, Belize. Ancient Mesoam 31, 175–187. https://doi.org/10.1017/S0956536119000233.

Awe, J.J., Helmke, C., Aimers, J.J., Ebert, C.E., Stemp, W.J., Hoggarth, J.A., 2020b. Applying regional, contextual, ethnohistoric and ethnographic approaches for understanding the significance of peri-abandonment deposits in western Belize. Ancient Mesoam 31, 109–126. https://doi.org/10.1017/S095653611900021X.

Bishop, R.L., 1994. Pre-columbian pottery: Research in the Maya region. In: Scott, D.A., Meyers, P. (Eds.), Archaeometry of Pre-columbian sites and artifacts. The Getty Conservation Institute, Los Angeles, pp. 15–65.

Bishop, R.L., 2014. Instrumental approaches to understanding Mesoamerican economy: Elusive promises. Ancient Mesoam 25, 251–269. https://doi.org/10.1017/S0956536114000157.

Bronk Ramsey, C., 2009. Bayesian analysis of radiocarbon dates. Radiocarbon 51, 337–360. https://doi.org/10.1017/S0033822200033865.

Callaghan, M.G., Pierce, D.E., Kovacevich, B., Glascock, M.D., 2017. Chemical paste characterization of Late Middle Preclassic-period ceramics from Holtun, Guatemala and its implications for production and exchange. J. Archaeol. Sci.: Rep. 12, 334–345. https://doi.org/10.1016/j.jasrep.2017.01.040.

Callaghan, M.G., Pierce, D.E., Gilstrap, W.D., 2018. The first Maya trade ware? New data on Middle Preclassic-period Mars Orange ware from Holtun, Guatemala. Lat. Am. Antiq. 12, 821–827. https://doi.org/10.1017/laq.2018.42.

Douglas, J.E., Brown, L.J., Awe, J.J., 2015. The final occupation: the Terminal Classic evidence from Plaza H, Cahal Pech. Belize. Res. Rep. in Belizean Archaeo. 12, 217–225.

Dussubieux, L., Robertshaw, P., Glascock, M.D., 2009. LA-ICP-MS analysis of African glass Leads: laboratory inter-comparison with an emphasis on the impact of corrosion on data interpretation. Int. J. of Mass Spectrom. 284, 152–161. https://doi.org/10.1016/j.ijms.2008.11.003.

Ebert, C.E., Culleton, B.J., Awe, J.J., Kennett, D.J., 2016. AMS ^{14}C dating of preclassic to classic period household construction in the Ancient Maya Community of Cahal Pech, Belize. Radiocarbon 58, 69–87. https://doi.org/10.1017/RDC.2015.7.

Ebert, C., Pierce, D., Awe, J., 2019. Preclassic ceramic economy in Belize: neutron activation analysis at Cahal Pech. Antiq. 93, 1266–1283. https://doi.org/10.15184/aqy.2019.93.

Fox, S., Awe, J.J., 2017. Ritual termination and ancestor reverence: the 2016 excavations at Structure 2, Zopilote. In: Ebert, C.E., Burke, C.C., Awe, J.J., Hoggarth, J.A. (Eds.), The Belize Valley Archaeological Reconnaissance Project: A Report of the 2016 Field Season. Baylor University, Waco, pp. 66–79.

Gaber, J.F., 2004. The Ancient Maya of the Belize Valley: A Half Century of Archaeological Research. University of Florida Press, Gainesville.

Garcia, K.L., 2008. Maya Pottery Specialization and Standardization: Using Late and Terminal Classic Ceramics from the Upper Belize River Valley to Evaluate Market Exchange. M.A. Thesis. University of Alabama, Tuscaloosa.

Gifford, J.C., 1976. Prehistoric Pottery Analysis and the Ceramics of Barton Ramie in the Belize Valley. Peabody Museum of Archaeology and Ethnology. Harvard University, Cambridge.

Glascock, M.D., Neff, H., 2003. Neutron activation analysis and provenance research in archaeology. Meas. Sci. Technol. 14 (9), 1516–1526. https://doi.org/10.1088/0957-0233/14/9/304.

Gratuze, B., Blet-Lemarquand, M., Barrandon, J.N., 2001. Mass spectrometry with laser sampling: a new tool to characterize archaeological materials. J. Radioanal. Nucl. Chem. 247 (3), 645–656.

Halperin, C.T., Bishop, R.L., 2016. Chemical analysis of Late Classic Maya polychrome pottery paints and pastes from Central Petén, Guatemala. J. Archaeo. Sci. 69, 118–129. https://doi.org/10.1016/j.jas.2016.04.007.

Helmke, C., Awe, J.J., 2012. Ancient Maya territorial organization of central Belize: confluence of archaeological and epigraphic data. Contrib. New World Archaeol. 4, 59–90.

Helmke, C., Awe, J.J., Grube, N., 2010. Carved Monuments and Inscriptions of Xunantunich: Implications for Terminal Classic Sociopolitical Relationships in the Belize Valley. In: LeCount, L.J., Yaeger, J. (Eds.), Classic Maya Provincial Politics: Xunantunich and Its Hinterlands. University of Arizona Press, Tucson, pp. 97–121.

Howie, L.A., 2005. Ceramic Production and Consumption in the Maya Lowlands during the Classic to Postclassic Transition: A Technological Study of Ceramics at Lamanai, Belize. Ph.D. Dissertation. University of Sheffield.

Johannesen, K., 2018. A Ceramic Analysis of Two Terminal Classic Maya Sites: Examining Economic Ties through Pottery. M.A. Thesis. University of Montana, Missoula.

Jordan, J.M., Hoggarth, J.A., Awe, J.J., 2020. Pottery, practice, and place: a communities of practice approach to commoner interaction in the Late to Terminal Classic Belize River Valley. J. Anthropol. Archaeol. 58 https://doi.org/10.1016/j.jaa.2020.101148.

LeCount, L.J., 2010. Mount Maloney people? Domestic pots, everyday practice, and the social formation of the Xunantunich polity. In: LeCount, L.J., Yaeger, J. (Eds.), Classic Maya Provincial Politics: Xunantunich and Its Hinterlands. University of Arizona Press, Tucson, pp. 209–230.

LeCount, L.J., Yaeger, J., Leventhal, R.M., Ashmore, W., 2002. Dating the rise and fall of Xunantunich. Belize. Anc. Mesoam. 13, 41–63. https://doi.org/10.1017/S0956536102131117.

LeCount, L.J., 1996. Pottery and Power: Feasting, Gifting, and Displaying Wealth Among the Late and Terminal Classic Lowland Maya. Ph.D. Dissertation. University Of California Los Angeles.

Miller, B.L., 1915. Graphite. The Mineral Industry, Its Statistics, Technology, and Trade. 23:371-382.

MURR Archaeometry Laboratory Database (n.d.) Available at: http://archaeometry.missouri. edu/datasets/datasets.html.

Pearce, N.J.G., Perkins, W.T., Westgate, J.A., Gorton, M.T., Jackson, S.E., Neal, C.R., Chenery, S.P., 1997. A compilation of new and published major and trace element data for NIST SRM 610 and SRM 612 glass reference materials, Geostand. Newsl., 21 (1):115-141. DOI:10.1111/j.1751-908X.1997.tb00538.x.

Shepard, A.O., 1939. Appendix B: Technological notes on the pottery of San Jose. In Thompson, J.E.S., Excavations at San Jose, British Honduras. Carnegie Institution of Washington Publication, No. 506. Carnegie Institution, Washington, D.C., pp. 251-277.

Shepard, A.O., 1956, Ceramics for Archaeologists. Carnegie Institution of Washington Publication; No. 609. Carnegie Institution, Washington, D.C.

Straight, K.D., 2017. A houseful of pots: applying ethnoarchaeological data to estimate annual ceramic vessel consumption rates of Classic Maya households. Anc. Mesoam. 28, 95–117. https://doi.org/10.1017/S0956536116000407.

Thompson, J.E.S., 1939. Excavations at San Jose, British Honduras. Carnegie Institution of Washington Publication, No. 506. Carnegie Institution, Washington, D.C.

Thompson, J.E.S. 1942. Late Ceramic Horizons at Benque Viejo, British Honduras. Contributions of American Anthropology and History, No. 35. Carnegie Institution, Washington D.C.

Thompson, R., 1958. Modern Yucatecan Maya pottery making. Memoirs of the Society for American Archaeology 15. Society for American Archaeology, Salt Lake City.

van der Weerd, J., Smith, G.D., Firth, S., Clark, R.J.H., 2004. Identification of black pigments on prehistoric Southwest American potsherds by infrared and Raman microscopy. J. Archaeo. Sci. 31 (10), 1429–1437. https://doi.org/10.1016/j.jas.2004.03.008.

Waksman, Y., 2017. Providence studies: productions and compositional groups. In: Hunt, A.M.W. (Ed.), The Oxford Handbook of Archaeological Ceramic Analysis. Oxford University Press, Oxford, pp. 148–162.

Zanotto, H.H., Awe, J.J., 2017. The Xunantunich archaeological and conservation project: A progress report of the second (2016) season of excavations. In: Ebert, C.E., Burke, C.C., Awe, J.J., Hoggarth, J.A. (Eds.), The Belize Valley Archaeological Reconnaissance Project: A Report of the 2016 Field Season. Baylor University, Waco, pp. 289–292.